Nucleic Acids Research, 2002, Vol. 30, No. 12 **2609–2619**

Properties of triple helices formed by parallel-stranded hairpins containing 8-aminopurines

Anna Aviñó, Miriam Frieden, Juan Carlos Morales[1], Beatriz García de la Torre[1], Ramón Güimil García[1], Ferran Azorín[1], José Luis Gelpí[2], Modesto Orozco[2], Carlos González[3] and Ramon Eritja[1,*]

Cygene Spain S.L., Parc Científic de Barcelona, Baldiri i Reixac 10-12, E-08028 Barcelona, Spain, [1]Institut de Biologia Molecular de Barcelona, C.S.I.C., Jordi Girona 18-26, E-08034 Barcelona, Spain, [2]Departament de Bioquímica i Biologia Molecular, Facultat de Química, Universitat de Barcelona, Martí i Franques 1, E-08028 Barcelona, Spain and [3]Instituto de Estructura de la Materia, C.S.I.C., Serrano 119, E-28006 Madrid, Spain

Received March 20, 2002; Revised and Accepted April 22, 2002

ABSTRACT

Parallel-stranded hairpins with a polypyrimidine sequence linked to a complementary purine carrying 8-aminopurines such as 8-aminoadenine, 8-aminoguanine and 8-aminohypoxanthine bind polypyrimidine sequences complementary (in an antiparallel sense) to the purine part by a triple helix. The relative stabilities of triplexes were assessed by UV-absorption melting experiments as a function of pH and salt concentration. Hairpins carrying 8-aminopurines give very stable triple helical structures even at neutral pH, as confirmed by gel-shift experiments, circular dichroism and nuclear magnetic resonance spectroscopy. The modified hairpins may be redesigned to cope with small interruptions in the polypyrimidine target sequence.

INTRODUCTION

Oligonucleotides bind in a sequence-specific manner to homopurine–homopyrimidine sequences of duplex and single-stranded DNA and RNA to form triplexes (1). Nucleic acid triplexes have wide applications in diagnosis, gene analysis and therapy, namely the extraction and purification of specific nucleotide sequences, control of gene expression, mapping of genomic DNA, induction of mutations in genomic DNA, detection of mutations in homopurine DNA sequences, site-directed mutagenesis, triplex-mediated inhibition of viral DNA integration, non-enzymatic ligation of double-helical DNA and quantification of polymerase chain reactions (1–5).

One of the main drawbacks of these applications is the low stability of triple helices especially in neutral conditions and when the homopurine–homopyrimidine tracks have interruptions. A large effort has been made to design modified oligonucleotides and thus enhance triple helix stability in homopolymers and triplexes with interruptions in the homopurine–homopyrimidine tracks (1,6,7). Successful modifications of the nucleobases include molecules such as 5-methylcytidine (8,9), 5-methyl-2,6(1H,3H)-pyrimidinedione (10) and 2′-*O*-methylpseudoisocytidine (11) among others (1–7).

Triplexes are typically formed by adding a triplex-forming oligonucleotide to duplex DNA. However, there is an alternative approach based on the use of parallel-stranded duplexes. Accordingly, purine residues are linked to a pyrimidine chain of inverted polarity by 3′-3′ or 5′-5′ internucleotide junctions (12). Such parallel-stranded DNA hairpins have been synthesized (12–14) and bind single-stranded DNA and RNA targets by triplex formation (12), similarly to the foldback all-pyrimidine hairpins described elsewhere (15,16).

Oligonucleotides containing 8-aminopurines may replace natural purines in triplexes (17–22). The introduction of an amino group at position 8 of adenine and guanine increases the stability of the triple helix owing to the combined effect of the gain in one Hoogsteen purine–pyrimidine H-bond (Fig. 1) and to the ability of the amino group to be integrated into the ‘spine of hydration’ located in the minor–major groove of the triplex structure (17,18,21,22). The preparation and binding properties of oligonucleotides containing 8-aminopurines has been reported elsewhere (17–22). However, natural oligonucleotides containing 8-aminopurines cannot be directly used for the specific binding of double-stranded DNA sequences, since the modified bases are purines that are in the target sequence and not in the Hoogsteen strand used for specific recognition of double-stranded DNA in usual triplex strategies.

We describe the binding properties of hairpins carrying 8-aminoadenine, 8-aminoguanine and 8-aminohypoxanthine connected head-to-head to the Hoogsteen pyrimidine strand (Fig. 1). Hairpins carrying 8-aminopurines form stable Hoogsteen parallel-stranded structures (23,24). Here we show that these modified hairpins bind to the Watson–Crick pyrimidine strand via a triple helix with greater affinity than hairpins containing only natural bases, especially in neutral conditions. The effect of pH, salt concentration and loop structure on triplex stability are analysed. Moreover, parallel-stranded hairpins are shown to form triplexes with a base interruption in the polypyrimidine target sequence. The increased stability of the triple helix at neutral conditions and the possibility to cope with the interruptions in the polypyrimidine target sequences

*To whom correspondence should be addressed. Tel: +34 93 4006145; Fax: +34 93 2045904; Email: recgma@cid.csic.es

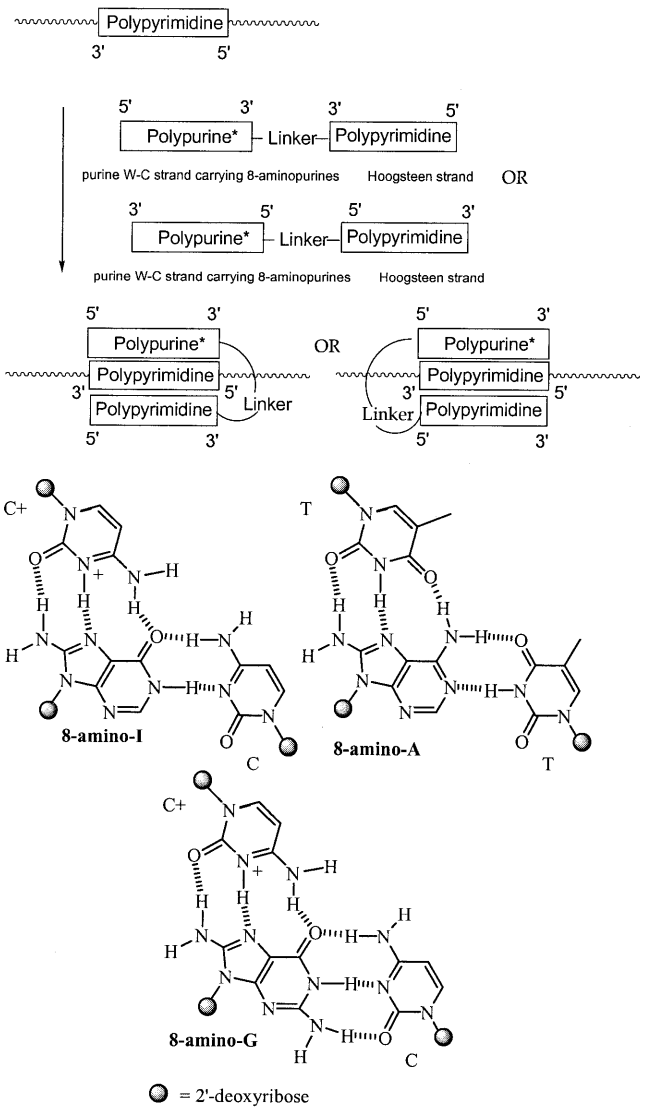

Figure 1. Scheme of binding a polypyrimidine single-stranded nucleic acid with the hairpins studied. Lower part, hypothetical base-pairing schemes of triads containing 8-aminopurines.

offer great potential for new applications based on triple helix formation such as structural studies, DNA-based diagnostic tools as well as antigene and antisense therapies (1–5).

MATERIALS AND METHODS

Preparation of hairpins containing 8-aminopurines

Oligonucleotides were prepared on an automatic Applied Biosystems 392 DNA synthesiser. The parallel-stranded hairpins were prepared as described elsewhere (12–14). 5′-5′ hairpins (R-22 derivatives) were prepared in three steps. First, the pyrimidine part was prepared using reversed C and T phosphoramidites and reversed C-support (linked to the support through the 5′ end). Second, a hexaethyleneglycol linker was added using a commercially available phosphoramidite. Third, the purine part carrying the modified 8-aminopurines was assembled using standard phosphoramidites for the natural bases and the 8-aminopurine phosphoramidites. The phosphoramidites of 8-aminoadenine, 8-aminoguanine and 8-aminohypoxanthine were prepared as described elsewhere (17–23). For the preparation of 3′-3′ hairpins (B-22 derivatives), a similar approach was used. In this case, the purine part was assembled first, followed by the hexaethyleneglycol. The pyrimidine part was the last to be assembled using reversed phosphoramidites. The phosphoramidite of protected 8-amino-2′-deoxyinosine was dissolved in dry dichloromethane to yield a 0.1 M solution. The remaining phosphoramidites were dissolved in dry acetonitrile (0.1 M solution). Oligonucleotides containing natural bases were prepared using commercially available chemicals and following standard protocols. After the assembly of the sequences, oligonucleotide-supports were treated with 32% aqueous ammonia at 55°C for 16 h except for oligonucleotides bearing 8-aminoguanine. In this case, a 0.1 M 2-mercaptoethanol solution in 32% aqueous ammonia was used and the treatment was extended to 24 h at 55°C (20). Ammoniacal solutions were concentrated to dryness and the products were purified by reversed-phase HPLC. Oligonucleotides were synthesised on a 0.2 µmol scale and with the last DMT group at the 5′ end (DMT on protocol) to facilitate reversed-phase purification. All purified products presented a major peak, which was collected. Yields (OD units at 260 nm after HPLC purification, 0.2 µmol) were between 5 and 10 OD. HPLC conditions, HPLC solutions were as follows: solvent A, 5% ACN in 100 mM triethylammonium acetate pH 6.5; and solvent B, 70% ACN in 100 mM triethylammonium acetate pH 6.5. Columns, PRP-1 (Hamilton), 250 × 10 mm; flow rate, 3 ml/min. A 30 min linear gradient from 10 to 80% B (DMT on) or a 30 min linear gradient from 0 to 50% B (DMT off).

Binding of hairpins to target sequences by melting experiments

Melting experiments with triple helices were performed as follows. Solutions of equimolar amounts of hairpins and the target Watson–Crick pyrimidine strand (11mer) were mixed in 0.1 M sodium phosphate/citric acid buffer of pH ranging from 5.5 to 7.0 with or without NaCl or $MgCl_2$. The DNA concentration was determined by UV absorbance measurements (260 nm) at 90°C using, for the DNA coil state, the following extinction coefficients: 7500, 8500, 12 500, 12 500, 15 000 and 15 000 M^{-1} cm^{-1} for C, T, G, 8-amino-G, A and 8-amino-A, respectively (8). The solutions were heated to 90°C, allowed to cool slowly to room temperature, and stored at 4°C until UV was measured. UV absorption spectra and melting experiments (absorbance versus temperature) were recorded in 1 cm path-length cells using a spectrophotometer, with a temperature controller and a programmed temperature increase rate of 0.5°C/min. Melting curves were run on duplex concentration of 4 µM at 260 nm.

The samples used for the thermodynamic studies were prepared in a similar way, but melting experiments were recorded at 260 nm using 0.1, 0.5 and 1 cm path-length cells.

Thermodynamic data were analysed as described elsewhere (8). Melting curves were obtained at concentrations ranging from 0.5 to 25 µM of triplex. The melting temperatures (T_m) were measured at the maximum of the first derivative of the melting curve. The plot of $1/T_m$ versus lnC was linear. Linear regression of the data gave the slope and the *y*-intercept, from

which ΔH and ΔS were obtained. The free energy was obtained from the standard equation: $\Delta G = \Delta H - T\Delta S$.

Binding of hairpins to target sequences by gel-shift experiments

The binding of hairpins to their polypyrimidine targets was analysed by gel retardation assays. The following targets were studied: WC-11mer, 5′-**TCT CCT CCT TC**-3′; and T31-PYR, 5′-CGA GTC ATT G**TC TCC TCC TTC** AGT CAT CGA G-3′.

Either the target oligonucleotides or the hairpins were radioactively labelled at the 5′ end by T4 polynucleotide kinase and [γ-^{32}P]ATP with 35–50 µmol of the oligonucleotide dissolved in 20 µl of kinase buffer. After incubation at 37°C for 45 min, the solution was heated to 70°C for 10 min to denature the enzyme then cooled to room temperature. An aliquot of 60 µl of 50 mM potassium acetate in ethanol was added to the solution and the mixture was left at –20°C for at least 3 h. The mixture was centrifuged at 4°C for 45 min (Eppendorf 5415D, 14 000 r.p.m.) and the supernatant removed. The pellet was washed with 60 µl of 80% ethanol and centrifuged for 20 min at 4°C. The supernatant was removed and the pellet was dissolved in 0.2 ml of water.

The radiolabelled target was incubated with the hairpins in 0.1 M sodium phosphate/citric acid buffer pH 5.5–7.0 at room temperature for 30–60 min. The hairpins were added in increasing amounts from 2 to 200 molar equivalents. After incubation, the mixtures were analysed by 15% polyacrylamide gel electrophoresis at room temperature using the same buffer as for the incubation: 0.1 M sodium phosphate/citric acid buffer pH 5.5–7.0. The formation of the triplex was monitored by the appearance of a radioactive band with less mobility than the band corresponding to the target alone.

Experiments carried out with radiolabelled hairpins were performed in a similar way. In this case, increasing amounts from 2 to 200 molar equivalents of target oligonucleotide were added to the hairpin.

Circular dichroism (CD)

Oligonucleotides were dissolved in 100 mM phosphate buffer pH 6.0, 50 mM NaCl and 10 mM $MgCl_2$. The equimolar concentration of each strand was 4–5 µM. The solutions were heated to 90°C, allowed to cool slowly to room temperature and stored at 4°C until CD was measured. The CD spectra were recorded on a Jasco J-720 spectropolarimeter attached to a Neslab RP-100 circulating water bath in 1 cm path-length quartz cylindrical cells. Spectra were recorded at room temperature using a 10 nm/min scan speed, a spectral band width of 1 nm and a time constant of 4 s. CD melting curves were recorded at 280 nm using a heating rate of 20°C/h and a scan speed of 100 nm/min. All the spectra were subtracted with the buffer blank, normalised to facilitate comparisons and noise reduced using Microcal Origin 5.0 software.

NMR spectroscopy

An equimolar mixture of hairpin d(3′-AG A^N GG A^N GGA AG-5′-$(EG)_6$-5′-CTT CCT CCT CT-3′) (A^N = 8-amino-A) and WC-11mer, 5′-TCT CCT CCT TC-3′, was prepared in 250 µl of 9:1 H_2O:D_2O, 25 mM sodium phosphate buffer and 100 mM NaCl. The pH was adjusted by adding small amounts of concentrated HCl. The final oligonucleotide concentration was ~1 mM. Spectra were acquired in a Bruker AMX spectrometer operating at 600 MHz and processed with the UXNMR software. Water suppression was performed using a jump-and-return pulse sequence with null excitation in the water signal (25). All experiments were carried out at 5°C.

Molecular modelling

Two types of theoretical calculations were made to test whether parallel-stranded hairpins behave as a template for triplex formation: (i) quantum mechanics and (ii) classical molecular dynamics.

Quantum mechanical calculations. The energy of the Watson–Crick hydrogen bonding of adenine (or 8-aminoadenine) and thymine, and guanine (or 8-aminoguanine) and cytosine was computed at the B3LYP/6-31G(d) level (26) for the isolated purines, and for the pre-formed Hoogsteen dimer adenine (or 8-aminoadenine) thymine or guanine (or 8-aminoguanine) cytosine$^+$ (Fig. 1). The geometries of monomers (A, A^N, G, G^N, C, T and C^+), dimers (A–T, A·T, A^N–T, A^N·T, G–C^+, G^N–C^+, G·C and G^N·C) and trimers (T–A·T, T–A^N·T, C^+–G·C and C^+–G^N·C) were fully optimised at the B3LYP/6-31G(d) level of theory (Watson–Crick base pair is indicated with a dot, Hoogsteen base pair is indicated with a dash). Optimised geometries were subjected to frequency analysis. Basis-set superposition errors (BSSE) were corrected following Boys and Bernardi (27).

Molecular dynamics. Trajectories for poly d(T–A·T), poly d(T–A) and poly(A·T) were obtained by classical molecular dynamics. Starting structures for our simulations were as described elsewhere (28,29) and then surrounded by cations to achieve neutrality, hydrated (around 2000–3000 molecules), optimised, thermalised and equilibrated following our standard multistage protocol (28,30). Simulations were carried out for 1.5 ns at constant pressure and temperature (P = 1 atm, T = 298°K) in periodic boundary conditions using the particle mesh Ewald technique [PBC-PME (31)]. Only the last 1 ns of the trajectories were considered for the analysis. SHAKE (32) was used to constrain all the bonds at optimum lengths, which allowed us to use a 2 fs time step for integration of Newton's laws. TIP3P (33) and AMBER-98 force-field (34,35), supplemented with specific parameters for protonated cytosine and 8-aminopurines (21,36) were used to describe molecular interactions.

Quantum mechanical calculations were made using the Gaussian-94 computer program. Molecular dynamic simulations were performed using the AMBER-95 suite of programs.

RESULTS AND DISCUSSION

Structure of the oligonucleotide derivatives

The binding properties of hairpins carrying 8-aminoadenine (A^N), 8-aminoguanine (G^N) and 8-aminohypoxanthine (I^N) connected head-to-head to the Hoogsteen pyrimidine strand were studied. The sequences of the oligonucleotides are shown in Figure 2. The target DNA sequence consist of a triplex characterised by Xodo and colleagues (8,37). Here, the polypyrimidine Hoogsteen strand was linked to the Watson–Crick polypurine strand.

R-22 $^{5'}$GAAGGAGGAGA$^{3'}$-(EG)$_6$-$^{3'}$TCTCCTCCTTC$^{5'}$

R-22A $^{5'}$GAAGG**A**^{N}GG**A**^{N}GA$^{3'}$-(EG)$_6$-$^{3'}$TCTCCTCCTTC$^{5'}$

R-22G $^{5'}$GAAG**G**^{N}AG**G**^{N}AGA$^{3'}$-(EG)$_6$-$^{3'}$TCTCCTCCTTC$^{5'}$

R-22I $^{5'}$GAAG**I**^{N}AG**I**^{N}AGA$^{3'}$-(EG)$_6$-$^{3'}$TCTCCTCCTTC$^{5'}$

B-22 $^{3'}$AGAGGAGGAAG$^{5'}$-(EG)$_6$-$^{5'}$CTTCCTCCTCT$^{3'}$

B-22A $^{3'}$AGA**A**^{N}GG**A**^{N}GGAAG$^{5'}$-(EG)$_6$-$^{5'}$CTTCCTCCTCT$^{3'}$

B-22G $^{3'}$AGA**G**^{N}GA**G**^{N}GAAG$^{5'}$-(EG)$_6$-$^{5'}$CTTCCTCCTCT$^{3'}$

B-22AG $^{3'}$AGA**A**^{N}**G**^{N}GA**A**^{N}**G**^{N}GAAG$^{5'}$-(EG)$_6$-$^{5'}$CTTCCTCCTCT$^{3'}$

B-22Acontrol $^{3'}$AGA**A**^{N}GG**A**^{N}GGAAG$^{5'}$-(EG)$_6$-$^{5'}$**TTTTTCCCCCC**$^{3'}$

B-22AMMT $^{3'}$AGA**A**^{N}GG**A**^{N}**C**GAAG$^{5'}$-(EG)$_6$-$^{5'}$CTTC**T**TCCTCT$^{3'}$

B-22AMMC $^{3'}$AGA**A**^{N}GG**A**^{N}**C**GAAG$^{5'}$-(EG)$_6$-$^{5'}$CTTC**C**TCCTCT$^{3'}$

B-22AMMG $^{3'}$AGA**A**^{N}GG**A**^{N}**C**GAAG$^{5'}$-(EG)$_6$-$^{5'}$CTTC**G**TCCTCT$^{3'}$

B-22AMMA $^{3'}$AGA**A**^{N}GG**A**^{N}**C**GAAG$^{5'}$-(EG)$_6$-$^{5'}$CTTC**A**TCCTCT$^{3'}$

B-22AMMpd $^{3'}$AGA**A**^{N}GG**A**^{N}**C**GAAG$^{5'}$-(EG)$_6$-$^{5'}$CTTC**pd**TCCTCT$^{3'}$

B-22AMMCA: $^{3'}$AGA**A**^{N}GG**A**^{N}**T**GAAG$^{5'}$-(EG)$_6$-$^{5'}$CTTC**C**TCCTCT$^{3'}$

B-22AMMTA: $^{3'}$AGA**A**^{N}GG**A**^{N}**T**GAAG$^{5'}$-(EG)$_6$-$^{5'}$CTTC**T**TCCTCT$^{3'}$

B-22AMMGA: $^{3'}$AGA**A**^{N}GG**A**^{N}**T**GAAG$^{5'}$-(EG)$_6$-$^{5'}$CTTC**G**TCCTCT$^{3'}$

B-22AMMAA: $^{3'}$AGA**A**^{N}GG**A**^{N}**T**GAAG$^{5'}$-(EG)$_6$-$^{5'}$CTTC**A**TCCTCT$^{3'}$

B-22AMMpdA: $^{3'}$AGA**A**^{N}GG**A**^{N}**T**GAAG$^{5'}$-(EG)$_6$-$^{5'}$CTTC**pd**TCCTCT$^{3'}$

B-22ALT1 $^{3'}$AGA**A**^{N}GG**A**^{N}GGAAG$^{5'}$-**$^{5'}$TTTT**-CTTCCTCCTCT$^{3'}$

B-22ALT2 $^{3'}$AGA**A**^{N}GG**A**^{N}GGAAG-**TTTT$^{5'}$**-$^{5'}$CTTCCTCCTCT$^{3'}$

B-22ALGA $^{3'}$AGA**A**^{N}GG**A**^{N}GGAAG-**GGAGG$^{5'}$**-$^{5'}$CTTCCTCCTCT$^{3'}$

B-22ALTG $^{3'}$AGA**A**^{N}GG**A**^{N}GGAAG-**CTTTG$^{5'}$**-$^{5'}$CTTCCTCCTCT$^{3'}$

Figure 2. Sequences of parallel-stranded hairpins carrying 8-aminopurines as prepared in this study; A^N, 8-aminoadenine; G^N, 8-aminoguanine; I^N, 8-aminohypoxanthine; $(EG)_6$, hexaethyleneglycol linker.

The first group of hairpins (R-22, R-22A, R-22G and R-22I) are parallel stranded and connected through their 3′ ends with a hexaethyleneglycol linker [$(EG)_6$]. They contain 22 bases and two purines replaced by the corresponding 8-aminopurines. In hairpin R-22A, two adenines are replaced by two 8-aminoadenines (A^N); in hairpin R-22G, two guanines are replaced by two 8-aminoguanines (G^N) and in hairpin R-22I, two guanines are substituted by two 8-aminohypoxanthines (I^N). Hairpin R-22 is a control sequence that contains only the natural bases without modification. The number of modified bases in each hairpin was selected to optimise stability with a minimum number of modified bases, as described elsewhere (17,21,22).

The second group of hairpins (B-22, B-22A and B-22G) have a similar composition but the polypurine and the polypyrimidine parts are connected through their 5′ ends with a hexaethyleneglycol linker [$(EG)_6$]. In addition, a hairpin bearing two 8-aminoguanines and two 8-aminoadenines was prepared (B-22AG) to test whether the stabilising properties of the two 8-aminopurines are additive. A control oligonucleotide (B-22Acontrol) with the same sequence in the polypurine part as B-22A but a random polypyrimidine sequence was prepared. Finally, the oligomers B-22AMMT, B-22AMMC, B-22AMMG, B-22AMMA, B-22AMMpd, B-22AMMCA, B-22AMMTA, B-22AMMGA, B-22AMMAA and B-22AMMpdA were prepared to study the effect of an interruption on the stability of the triple helix. In these hairpins, two adenines are replaced by two 8-aminoadenines. A pyrimidine (C or T) is located in the middle position of the purine part, and each of the natural bases and an abasic site model compound (propanediol, pd) are located in the corresponding position at the Hoogsteen strand.

A third group of oligomers (B-22ALT1, B-22ALT2, B-22ALGA, B-22ALTG and B-22N) have the same nucleotide sequence as B-22A but the loop between the polypurine and polypyrimidine parts are made out of nucleotides [-TTTT- (8), -GGAGG- (12), -CTTTG- (38)] instead of the hexaethyleneglycol bridge (16).

Table 1. Melting temperatures[a] (°C) for the triplex formed by R-22 derivatives and WC-11mer

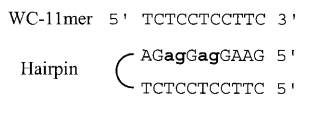

Hairpin	Target	pH 4.5	pH 5.5	pH 6.0	pH 6.5	pH 7.0
R-22	WC-11mer	69	56	47	36	32
R-22A	WC-11mer	73	62	56	48	45
R-22G	WC-11mer	76	67	59	53	51
R-22I	WC-11mer	65	34, 55	20, 46	40	38

[a]1 M NaCl, 100 mM sodium phosphate/citric acid buffer.

Thermal stability of the triplex formed by hairpins linked by 3′-3′ bonds

The relative stability of triple helices formed by R-22 hairpin derivatives and the polypyrimidine target sequence (WC-11mer) was measured spectrophotometrically at various pHs (pH 4.5–7.0). In almost all cases, one single transition was observed with a hyperchromicity ~25% at acidic pH and 20% at neutral pH. The melting curve was assigned to the transition from triple helix to random coil. Exceptionally, the melting curve of the triplex R-22I–WC-11mer at pH 5.5 and 6 showed two pH-dependent transitions. When A and G were replaced by 8-aminoadenine (A^N) and 8-aminoguanine (G^N) in the triple helix, this was greatly stabilised (10–18°C in the range pH 4.5–7.0, Table 1). When guanine was replaced by 8-aminohypoxanthine (I^N) triple helix stability increased only slightly at acidic pH, but the triplex containing I^N maintained its stability at neutral pH while the unmodified triplex stability rapidly decreased.

To test whether transition was due to triple helix formation, melting curves were obtained with hairpins (R-22, R-22A, R-22G and R-22I) alone, in the absence of the polypyrimidine target sequence (WC-11mer). A single transition was also observed but at lower temperature and with a hyperchromicity ~10–15%, indicating that the transition observed with the WC-11mer (triple helix) differs from that observed without the WC-11mer. The transition observed in the hairpins alone corresponds to the parallel duplex to random coil transition (23).

Hairpins linked by 3′-3′ bonds versus hairpins with 5′-5′ linkages

In addition to the hairpins linked by 3′-3′ bonds (R-22 derivatives), hairpins linked by 5′-5′ bonds (B-22 derivatives) were

Table 2. Melting temperatures[a] (°C) for the triplex formed by B-22 derivatives and WC-11mer

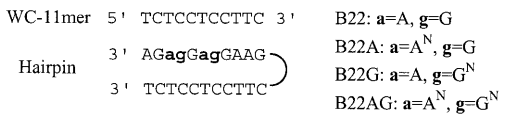

Hairpin	Target	pH 4.6	pH 5.5	pH 6.0	pH 6.5	pH 7.0
B-22	WC-11mer	63	54	45	33	20
B-22A	WC-11mer	73	57	51	43	34
B-22G	WC-11mer	75	69	59	50	40
B-22AG	WC-11mer	80	71	65	56	53

[a]1 M NaCl, 100 mM sodium phosphate/citric acid buffer.

prepared. The relative stability of triple helices formed by the B-22 oligonucleotide derivatives and the polypyrimidine target sequence (WC-11mer) was measured. As described above, one single transition was observed with a hyperchromicity ~25%, which was assigned to the melting of the triple helix. Replacement of A by 8-aminoadenine (A^N) and guanine by 8-aminoguanine (G^N) in triple helix greatly stabilised the triple helix (Table 2). Moreover, when the melting curves of the hairpins were analysed without the target WC-11mer, the parallel structure was stabilised by the presence of 8-aminopurines (23). At acidic pH triplexes formed by both types of hairpins have similar stability. At neutral pH hairpins linked by 3′-3′ bonds (R-22 derivatives) form more stable triplexes than hairpins linked by 5′-5′ bonds (B-22 derivatives). Nevertheless, the increase in stability due to 8-aminopurines was similar in both systems.

Next, we examined whether the stabilisation properties of 8-aminoadenine and 8-aminoguanine are additive. A hairpin with two 8-aminoadenine and two 8-aminoguanine substitutions was prepared (B22AG). Melting curves were obtained with the appropriate hairpin and the target WC-11mer at pHs between 4.5 and 7.0, 0.1 M sodium phosphate/citric acid, 1 M NaCl. We found that the stabilisation properties of the 8-aminopurines are additive (Table 2). For example, at pH 6.0 the addition of the two 8-aminoguanines and two 8-aminoadenines raises the melting temperature by 20°C, whereas two 8-aminoadenines induce an increase of 6°C, and two 8-aminoguanines a rise of 14°C.

Role of the Hoogsteen strand on the triplex formation of hairpins

The role of the Hoogsteen strand was further investigated. We prepared a hairpin probe of the same purine sequence, but with two 8-aminoadenine substitutions and a non-complementary pyrimidine strand. This oligonucleotide (named B-22Acontrol) can only form Watson–Crick interactions with the target sequence (WC-11mer).

When the Hoogsteen strand is replaced by a non-complementary sequence, the structure of the parallel duplex is lost, as revealed by the disappearance of the transition observed when the melting curve is obtained without the target WC-11mer (Table 3).

The transitions observed with the duplexes formed by B22-Acontrol–WC-11mer showed lower T_m and hyperchromicity. The hyperchromicity associated with the transition of the duplex formed by B-22Acontrol–WC-11mer was 11%, which is indicative of a duplex-to-single-strand transition.

The transitions observed with the complex formed by the B22A–WC-11mer showed a 22% hyperchromicity, indicating a triplex-to-single-strand transition. The difference between the T_m of the B-22Acontrol duplex and B-22A triplex is the gain obtained by the addition of the Hoogsteen strand. At pH 6.0, this difference is of 11°C (1.0°C per base) and at pH 5.5, it is of 16°C (1.4°C per base).

Salts effects on triplex stability

Next, we studied the effect of NaCl, $MgCl_2$ and spermine on the stability of triplexes at pH 6.0. We used the triplex formed by the hairpin B-22A and the WC-11mer, as well as the triplex formed by the hairpin B-22G and the WC-11mer. For NaCl, the buffer used was 0.1 M sodium phosphate/citric acid pH 6.0. For $MgCl_2$ and spermine, the buffer used was 0.1 M sodium phosphate pH 6.0.

Sodium chloride had a slight stabilisation effect [from 49°C (without NaCl) to 51°C (1 M NaCl), see Supplementary Material]. Low concentrations of $MgCl_2$ stabilise the triplex, e.g. the melting temperature of triplexes B-22G–WC-11mer and B-22A–WC-11mer increased by 5°C from 0 to 10 mM $MgCl_2$ (see Supplementary Material). From 10 to 50 mM $MgCl_2$, the increase in melting temperature is 0 or <1°C. In conclusion, the presence of magnesium is slightly beneficial for the stability of the triplex, 10 mM being the optimal concentration. Spermine hardly affects the stability of triplexes.

Table 3. Effect of the Hoogsteen strand

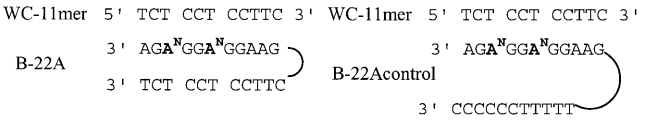

Hairpin	Target	pH 5.5, 1 M NaCl		pH 6.0, 1 M NaCl	
		T_m (°C)	Hyperchromicity	T_m (°C)	Hyperchromicity
B-22Acontrol	WC-11mer	41	+12% (duplex to ss)	40	+11% (duplex to ss)
B-22Acontrol	None	No transition		No transition	
B-22A	WC-11mer	57	+22% (triplex to ss)	51	+20% (triplex to ss)
B-22A	None	47	+12% (duplex to ss)	38	+11% (duplex to ss)

Table 4. Melting temperatures of triplex containing one interruption at the polypurine/polypyrimidine track (at pH 6.0, 0.1 M sodium phosphate and citric acid, 1 M NaCl)

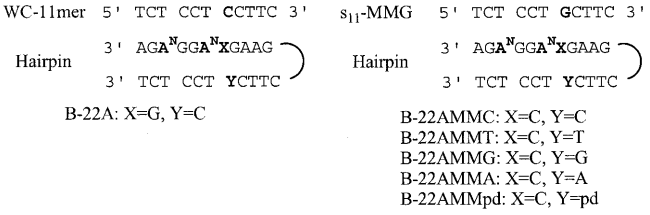

Hairpin	Target 1, WC-11mer		Target 2, s_{11}-MMG	
	Triad 1[a]	T_m (°C)	Triad 2[a]	T_m (°C)
B-22A	C·G–C	51	G·G–C	43
B-22AMMC	C·C–C	33	G·C–C	47
B-22AMMT	C·C–T	30	G·C–T	45
B-22AMMG	C·C–G	34	G·C–G	43
B-22AMMA	C·C–A	28	G·C–A	41
B-22AMMpd	C·C–pd	29	G·C–pd	44

[a]Watson–Crick base pair is indicated with a dot, Hoogsteen pair is indicated with a dash.

Table 5. Melting temperatures of triplex containing one interruption at the polypurine/polypyrimidine track (at pH 6.0, 0.1 M sodium phosphate and citric acid, 1 M NaCl)

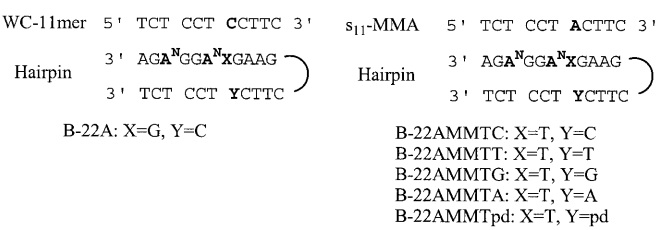

Hairpin	Target 1, WC-11mer		Target 2, s_{11}-MMA	
	Triad 1[a]	T_m (°C)	Triad 2[a]	T_m (°C)
B-22A	C·G–C	51	G·G–C	43
B-22AMMTC	C·T–C	28	A·T–C	39
B-22AMMTT	C·T–T	31	A·T–T	40
B-22AMMTG	C·T–G	33	A·T–G	46
B-22AMMTA	C·T–A	31	A·T–A	40
B-22AMMTp	C·T–pd	30	A·T–pd	42

[a]Watson–Crick base pair is indicated with a dot, Hoogsteen pair is indicated with a dash.

Presence of interruptions in the polypyrimidine target sequence

We also aimed to assess the effect of an interruption on the polypyrimidine track of the target. To this end, two polypyrimidine targets with a purine in the middle of the sequence were prepared (s_{11}-MMG, 5′-TCT CCT **G**CT TC-3′ and s_{11}-MMA, 5′-TCT CCT **A**CT TC-3′). Next, hairpins carrying the four natural bases and the abasic model compound, pd, at the Hoogsteen position were prepared (Fig. 2). Moreover, two 8-aminoadenines were introduced in the purine part. These oligomers have the complementary base at the Watson–Crick position opposite to the interruption and a T, C, G, A or pd on the Hoogsteen strand opposite to the interruption. Melting curves were obtained at pH 6.0, 0.1 M sodium phosphate, 1 M NaCl.

The melting temperatures of triplexes carrying a guanine on the polypyrimidine target instead of a cytosine are shown in Table 4. The hairpin with a cytosine in the Hoogsteen pyrimidine part gave the best binding. Hairpin B-22AMMC bound to its target (s_{11}-MMG), although the T_m decreased by 4°C (47°C B-22AMMC–s_{11}-MM compared with 51°C B-22A–WC-11mer). The binding of the new hairpin to its new target is very selective as revealed by the marked decrease in the T_m of the triplex B-22AMMC with the old target (33°C B-22AMMC–WC-11mer versus 47°C B-22AMMC–s_{11}-MMG).

A similar result was obtained when an adenine was introduced in the polypyrimidine target (Table 5). In this case, the best base at the Hoogsteen position was G. The preference of G to bind to A·T interruptions and the preference of C to bind G·C interruptions are well documented (39). However, we would like to underline that interruptions in parallel hairpins are easier to overcome thanks to the purine Watson–Crick part. Thus parallel hairpins, especially hairpins carrying 8-aminopurines, can be redesigned to bind efficiently to polypyrimidine targets carrying a short interruption.

Role of the loop on triplex stability

Finally, the role of the loop on the stability of the triplex was analysed by preparing derivatives of B-22A with various loops. In addition to the hexaethyleneglycol linker, the nucleotide loops -TTTT- (8), -GGAGG- (12) and -CTTTG- (38) were studied. Two tetrathymine loops were prepared: one oppositely oriented to the purine strand (B-22ALT1) and the second in the same orientation as the purine strand (B-22ALT2). The GGAAA and CTTTG loops were in the same orientation as the purine strand (B-22ALGA and B-22ALTG). The melting curves of triplexes formed by hairpins and target WC-11mer were obtained at pH 6.0, 0.1 M sodium phosphate, 1 M NaCl. Melting temperatures are as shown: B-22A, 3′-AGA^{N}GGA^{N}GGAAG-5′-**(EG)$_6$**-5′-CTTCCTCCTCT-3′, T_m = 51°C; B-22ALT1, 3′-AGA^{N}G-GA^{N}GGAAG-5′-5′-**TTTT**-CTTCCTCCTCT-3′, T_m = 57°C; B-22ALT2, 3′-AGA^{N}GGA^{N}GGAAG-**TTTT**-5′-5′-CTTCCT-CCTCT-3′, T_m = 55°C; B-22ALGA, 3′-AGA^{N}GGA^{N}GGAAG-**GGAGG**-5′-5′-CTTCCTCCTCT-3′, T_m = 54°C; B-22ALTG, 3′-AGA^{N}GGA^{N}GGAAG-**CTTTG**-5′-5′-CTTCCTCCTCT-3′, T_m = 54°C.

Nucleotide loops are slightly more suitable for the stability of the triplex than the hexaethyleneglycol linker. Best results were obtained with the reversed TTTT linker (hairpin B-22ALT1, ΔT_m 6°C), followed by the TTTT linker (hairpin B-22ALT2, ΔT_m 4°C) and the GGAGG and CTTTG linkers (hairpin B-22ALGA, B-22ALTG, ΔT_m 3°C). We suggest that the enhanced stability found with hairpins having nucleotide loops is due to the high salt concentrations used in the melting experiments. When melting experiments were performed at lower salt concentrations, the differences between hairpins

Table 6. Folding processes and associated energies (in kcal/mol) computed in the gas phase at the B3LYP/6-31G(d) level of theory

Folding process	Folding energy
A + T → A·T	–12.1
A^N + T → A^N·T	–11.9
G + C → G·C	–25.1
G^N + C → G^N·C	–24.8
(T–A) + T → T–A·T	–10.8
(T–A^N) + T → T–A^N·T	–11.6
(C^+–G) + C → C^+–G·C	–28.1
(C^+–G^N) + C → C^+–G^N·C	–27.0

Watson–Crick base pair is indicated with a dot, Hoogsteen base pair is indicated with a dash.

with the hexaethyleneglycol linker and nucleotide linkers were less pronounced (data not shown).

Molecular modelling

The formation of a triple helix by the binding of a Hoogsteen parallel-stranded duplex to a single-stranded oligonucleotide is guided by the formation of Watson–Crick-like H-bonds. The presence of the complementary Hoogsteen base may alter the magnitude of the Watson–Crick interaction. Results in Table 6 demonstrate that no dramatic changes can be expected in the Watson–Crick interaction by the presence of the Hoogsteen base pair. Thus, the binding of T to the Hoogsteen A–T (or A^N–T) dimer is <1 kcal/mol worse than the binding to A and the binding of C to the protonated Hoogsteen dimer G–C (or G^N–C) is 2–3 kcal/mol better than the binding to an isolated G. The presence of 8-aminopurines might slightly decrease in the intensity of Watson–Crick interactions, but without affecting the formation of triplexes from Hoogsteen duplexes, as reported elsewhere (17,21,40).

Theoretical calculations suggest that a pre-organised Hoogsteen duplex can give rise to a triplex. However, the isolated Hoogsteen duplex may not be sufficiently pre-organised. The magnitude of the pre-organisation work can be estimated by the mean root mean squared deviation (RMSd) between the structures sampled during the trajectories of the isolated duplex and the average structure of the duplex in the triplex structure. Figure 3 displays the RMSd between the trajectories of both Watson–Crick and Hoogsteen duplexes and the average structures of both duplexes when incorporated inside the triplex [average structure obtained by analysis of the molecular dynamics (MD) trajectory of the triplex]. The RMSd between the free Hoogsteen and the triplex pre-organised Hoogsteen duplex is only ~1 Å, near the thermal noise of the simulation, as revealed by the fact that the RMSd between the trajectories of the isolated duplexes (Hoogsteen or Watson–Crick) and the corresponding MD-averaged structures is ~0.8 Å. In contrast, the RMSd between the free Watson–Crick duplex and the triplex pre-organised Watson–Crick duplex is ~2 Å. In summary, MD simulations strongly suggest that the free parallel Hoogsteen duplex is better pre-organised to form a triplex than the Watson–Crick antiparallel duplex. This theoretical finding agrees with the CD data, which show that the spectra changes more in the transition

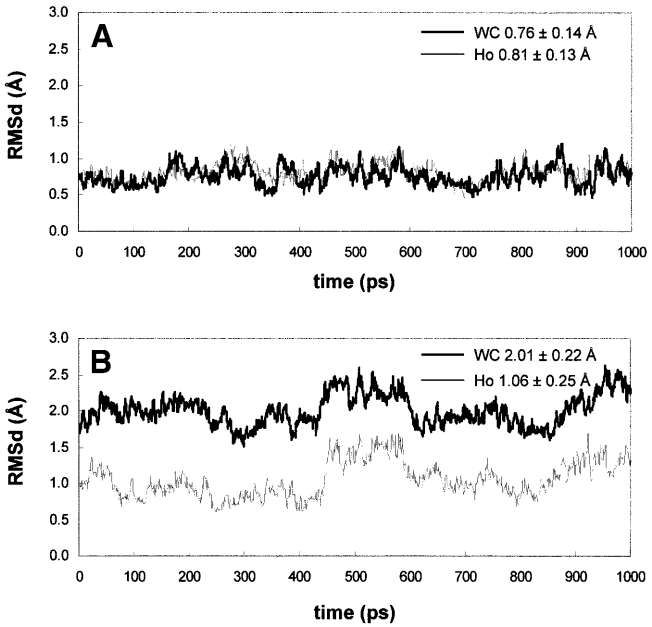

Figure 3. RMSds in Å between the trajectories of the parallel Hoogsteen (Ho) and antiparallel Watson–Crick (WC) duplexes and their respective MD-averaged structures (top), and between the same trajectories and the MD-averaged structures of both duplexes in the antiparallel triplex (bottom). Bases at both ends were removed for RMSd calculations.

from a Watson–Crick duplex to triplex than in the transition from a Hoogsteen duplex to the corresponding triplex (41,42).

In summary, the bulk of theoretical calculations strongly support that the Hoogsteen parallel hairpins can be a very efficient template for the formation of triple helices.

Thermodynamic studies

The dependence of the triplex to random coil transition on DNA concentration was studied on several triplexes (Table 7). In all cases, the melting temperatures of the triplex to random coil transitions decrease with the concentration, as expected for a bimolecular transition. The plot of $1/T_m$ versus ln concentration was linear, giving a slope and a *y*-intercept from which ΔH, ΔS and ΔG were obtained (Table 7).

The ΔG for the triplex dissociation was –58 kJ/mol for the unmodified triplex, –76 kJ/mol for the triplexes carrying two A^N and –88 kJ/mol for the triplex carrying two G^N. Comparison between these values gives a difference in ΔG of ~17 kJ/mol for two A→A^N substitutions (7.5 kJ/mol, 2.0 kcal/mol per substitution). For the triplex carrying G^N, the difference in ΔG is 30 kJ/mol (15 kJ/mol, 3.6 kcal/mol per substitution). Compared with other base analogues, these are among the highest triplex stabilisation properties reported for a modified base, although we measured the stability of Hoogsteen and Watson–Crick base pairs jointly.

Gel-shift assays

The binding of hairpins to their targets was also analysed by gel-shift experiments. The target was labelled radioactively with [γ-^{32}P]ATP and polynucleotide kinase and increasing amounts of the hairpins were added. After incubation at room temperature for 0.5–1 h in a citric/phosphate buffer pH 6 of 100 mM Na^+ ionic strength, the mixtures were analysed by

Table 7. Thermodynamic parameters for triplex to random coil transitions in sodium acetate 100 mM (pH 6.0), 50 mM NaCl, 10 mM $MgCl_2$ from the slope of the plot $1/T_m$ versus ln C[a]

Triplex	T_m (°C)[b]	ΔH (kJ/mol)	ΔS (J/mol K)	ΔG (kJ/mol)
B-22 + WC-11mer	34.5	–731	–2258	–58
B-22A + WC-11mer	52.5	–498	–1416	–76
B-22G + WC-11mer	57.3	–554	–1562	–88

[a]ΔH, ΔS and ΔG are given as round numbers, ΔG is calculated at 25°C, with the assumption that ΔH and ΔS do not depend on temperature; analysis has been carried out using melting temperatures obtained from denaturation curves; error on T_m is 0.7°C.
[b]At 4 µM triplex concentration.

polyacrylamide gel electrophoresis. The formation of the triplex was monitored by the appearance of a radioactive band with less mobility than the band corresponding to the target alone (Fig. 4).

Figure 4 shows the binding of hairpins R-22, R-22A and R-22G to the single-stranded target WC-11mer (5′-TCTC-CTCCTTC-3′). In all cases, a new radioactive band with lower mobility appeared. The relative intensity of this new band is consistent with the melting experiments. For example, the hairpins carrying the modified purines (A^N and G^N) completed the formation of the new band at a lower concentration (0.02–0.1 µM, Fig. 4) than the unmodified hairpin (0.5 µM, Fig. 4). The hairpin carrying G^N also showed better binding properties than the hairpin carrying A^N, in agreement with melting experiments. Moreover, binding is more efficient at pH 5.0 than at pH 7.0 (data not shown). We also found that the binding of hairpin B-22Acontrol, which had a non-functional Hoogsteen strand, with its target WC-11mer gave a low mobility band but at concentrations 100-fold higher than hairpin B-22A (data not shown). All these data indicate that the lower mobility bands detected with hairpins correspond to the triplex.

The binding of hairpin R-22G to the single-stranded target WC-11mer and a double-stranded target formed by the WC-11mer (5′-TCTCCTCCTTC-3′) and its complementary purine strand (3′-AGAGGAGGAAG-5′) was also examined. When the labelled oligonucleotide is the target pyrimidine strand (WC-11mer) a new radioactive band with lower mobility appears in both single and double-stranded targets, revealing the formation of the triplex (see Supplementary Material). In contrast, when the labelled oligonucleotide is the purine strand, no new band is observed, indicating that hairpins only bind to the target pyrimidine strand.

In addition, we studied the binding of hairpins to a second set of single and double-stranded DNA targets longer than 11 bases. The double-stranded DNA target had 31 bp containing an 11 base pyrimidine track complementary to the hairpins described in this study at the middle of the molecule:

T_{31} 5′-CGAGTCATTG**TCTCCTCCTTC**AGTCATCGAG-3′
T_{31} compl. 3′-GCTCAGTAAC**AGAGGAGGAAG**TCAGT-AGCTC-5′

The binding of hairpins to single-stranded targets (T_{31}) was clearly detected (Fig. 5). In contrast, hairpins did not bind to double-stranded DNA (data not shown). The differences in binding on double-stranded DNA targets may be due to the fact that small duplexes contain a large population of

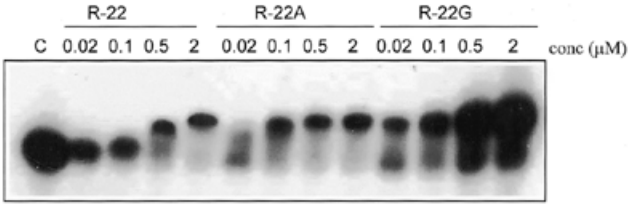

Figure 4. Binding of R-22, R-22A and R-22G to WC-11mer (citric/phosphate buffer pH 6 of 100 mM Na^+ ionic strength). Radiolabelled DNA target (10 nmol) was incubated at room temperature with 2–200 equivalents of cold hairpins R-22, R-22A and R-22G and the mixtures were analysed by 15% native polyacrylamide gel electrophoresis at room temperature.

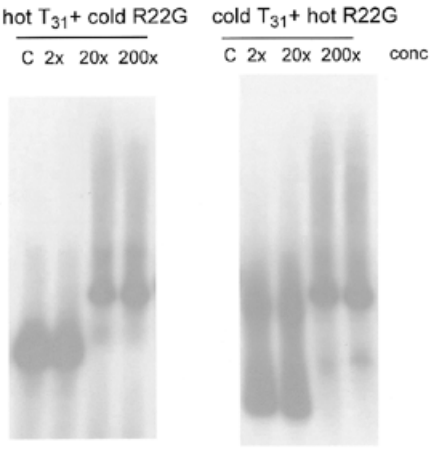

Figure 5. Binding of hairpin R-22G to single-stranded target T_{31} at pH 5.0. Left, the ^{32}P-labelled oligonucleotide was the target T_{31} and increasing (2×, 20×, 200×) amounts of cold B-22G were added. Right, the ^{32}P-labelled oligonucleotide was the hairpin R-22G and increasing (2×, 20×, 200×) amounts of cold T_{31} were added. Incubation time, 1 h at room temperature.

single-stranded molecules in equilibrium with the double-stranded form. The hairpin probably binds the single-stranded form, thus displacing the double-stranded form to the triplex. In longer duplexes, single-stranded forms are scarce, and so the hairpin has to bind and open the duplex to displace the complementary strand. For the hairpins described in this study, this phenomenon may be very slow or impracticable. A more detailed study should be performed to confirm these hypotheses.

When the binding experiment was performed by addition of excess of cold target T_{31} to radiolabelled hairpin (R22G), triplex formation was also observed (Fig. 5). Radiolabelled hairpin (R22G) alone showed two bands in native gels. The fast running band showed the mobility expected for an oligonucleotide of 22 bases. The slow running band had the mobility of a dimer. It is believed that this second band corresponds to the parallel dimer. Thus parallel hairpins are in equilibrium between the intramolecular hairpin and the intermolecular dimer. When the polypyrimidine target was added, the mobility of the dimer varied enough to show complete formation of the band corresponding to the triplex. Formation of the triplex of the parallel dimer was not observed.

Circular dichroism

To confirm triplex formation and gain more information on the structure of the hairpins, CD spectra were obtained. This

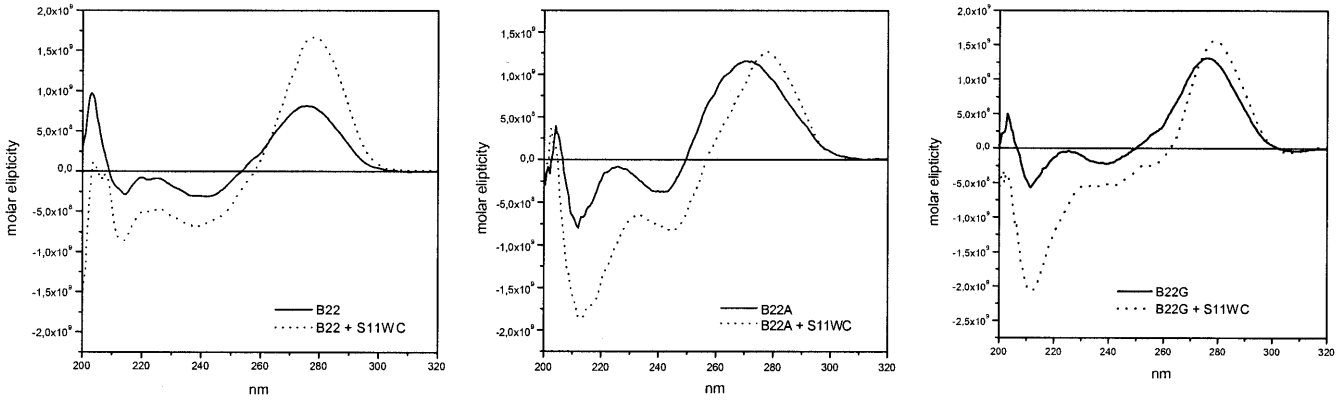

Figure 6. CD spectra of hairpins B-22, B-22G and B-22A alone and together with their pyrimidine target WC-11mer (50 mM NaCl, 10 mM $MgCl_2$, 0.1 M sodium phosphate pH 6).

technique measures the differences in the absorption of polarised light. Changes in the conformation of nucleic acids can be detected by CD and comparison of the spectra with the spectra of known structures suggests the presence of a particular conformation. The appearance of an intense negative short-wavelength (210–220 nm) band in the CD spectra indicates the formation of a triple-stranded complex (39,41,42). The CD spectra of the triplex formed between the hairpins (B-22, B-22A and B-22G) and their targets as well as the CD spectra of the hairpins alone are shown in Figure 6. In all cases, we observed an intense negative band (near 215 nm) upon binding of the hairpins with the target molecule. The intensity of the negative band correlates with the strength of the interactions because the negative band is more intense with the triplex formed by modified hairpins (B-22A and B-22G) which are more stable by melting experiments.

The melting curves of triplexes formed by hairpins B-22A and B-22G with their polypyrimidine target (WC-11mer) were also analysed by CD spectrometry. Melting temperatures obtained by CD experiments were similar to temperatures observed by UV absorption (53.0°C for triplex B-22A–WC-11mer; 56.5°C for triplex B-22G–WC-11mer in 50 mM NaCl, 10 mM $MgCl_2$, 0.1 M sodium phosphate pH 6.0).

NMR spectra

The imino region of one-dimensional ^{1}H-NMR spectra of the triplex formed by hairpin B-22A and polypyrimidine target WC-11mer at two pHs is shown in Figure 7. Most of the expected imino proton signals are clearly observed between 12 and 16 p.p.m. The presence of four imino signals between 15 and 16.0 p.p.m. clearly indicates that cytosines are protonated. The spectrum is consistent with a triple helix. Finally, we would like to highlight that most of the features of the exchangeable proton spectra are observed at pH 6.6, which points to the high stability of the triplex at neutral pH.

Interestingly, the lines of the exchangeable protons in this triplex are much narrower than in the isolated B-22A hairpin (see figure 10 in ref. 23). The line-broadening in the parallel Hoogsteen hairpin may be due to a conformational or solvent exchange. This dynamic effect is not observed upon triplex formation.

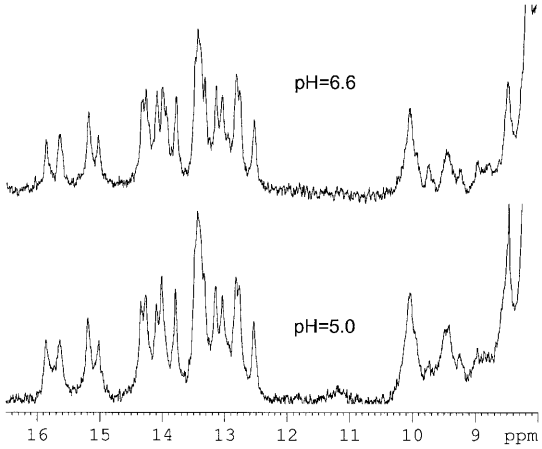

Figure 7. Exchangeable proton region of the NMR spectra of triplex formed by B22A: d[3′-AGA^{N}GGA^{N}GGAAG-5′-$(EG)_6$-5′-CTTCCTCCTCT-3′] and WC-11mer (3′-CTTCCTCCTCT-5′) at T = 5°C.

CONCLUSIONS

The triplex stabilisation binding properties of parallel-stranded hairpins carrying 8-aminopurines were evaluated by melting, gel-shift, CD and NMR experiments. These hairpins bind specific single-stranded polypyrimidine targets via triplex formation. The binding of these hairpins is stronger when they contain 8-aminopurines. 8-Aminoguanine showed the strongest stabilising effect, followed by 8-aminoadenine. 8-Aminohypoxanthine is more efficient than guanine only at neutral pH. The stability of the triplex formed by hairpins carrying 8-aminopurines is pH dependent but the interaction of the modified hairpins with their target is so strong that triplexes are observed even at neutral pH on a short model sequence consisting of only of 11 bases. Both 8-aminoadenine and 8-aminoguanine have an additive effect on the stability of the triplex. The loop that connects the homopurine sequence with the homopyrimidine sequence may also have an additional stabilising effect if it is made of nucleotides.

The modified hairpins may be redesigned to cope with small interruptions in the polypyrimidine target sequence. This offers great potential for applications in the triplex field,

especially for single-stranded targets, e.g. in antisense field and RNA detection. The use of 8-aminopurines is also compatible with most of the developments described in the triplex field so we believe that 8-aminopurines will improve any existing methodology based on triplex formation (1–11).

SUPPLEMENTARY MATERIAL

Supplementary Material is available at NAR Online. Table S1 shows melting temperatures of triplexes formed by hairpins B-22A and B-22G at various salt concentrations. Figure S1 shows the binding of hairpin R-22G to single- and double-stranded targets by gel-shift experiments. Figure S2 shows the melting experiment on the triplex formed by B-22G and WC-11mer followed by CD.

ACKNOWLEDGEMENTS

We thank the Dirección General de Investigación Científica y Técnica (grants PB98-1222, PM99-0046, BQU2000-0649 and CAL01-058-C2-2), the Generalitat de Catalunya (2000-SGR-0018 and 2001-SGR-0049) and Cygene Inc. for financial support.

REFERENCES

1. Thuong,N.T. and Hélène,C. (1993) Sequence-specific recognition and modification of double-helical DNA by oligonucleotides. *Angew. Chem. Int. Ed. Engl.*, **32**, 666–690.
2. Chan,P.P. and Glazer,P.M. (1997) Triplex DNA: fundamentals, advances and potential applications for gene therapy. *J. Mol. Med.*, **75**, 267–282.
3. Vazquez,K. and Wilson,J.H. (1998) Triplex-directed modification of genes and gene activity. *Trends Biochem. Sci.*, **23**, 4–9.
4. Soyfer,V.N. and Potaman,V.N. (1996) *Triple Helical Nucleic Acids.* Springer-Verlag, New York.
5. Malvy,C., Harel-Bellan,A. and Pritchard,L.L. (1999) *Triple Helix Forming Oligonucleotides.* Kluwer Academic Publishers, Dordrecht, The Netherlands.
6. Robles,J., Grandas,A., Pedroso,E., Luque,F.J., Eritja,R. and Orozco,M. (2002) Nucleic acid triple helices: stability effects of nucleobase modifications. *Curr. Org. Chem.*, in press.
7. Luyten,I. and Herdewijn,P. (1998) Hybridization properties of base-modified oligonucleotides within the double and triple helix motif. *Eur. J. Med. Chem.*, **33**, 515–576.
8. Xodo,L.E., Manzini,G., Quadrifolio,F., van der Marel,G.A. and van Boom,J.H. (1991) Effect of 5-methylcytosine on the stability of triple-stranded DNA—a thermodynamic study. *Nucleic Acids Res.,* **19**, 5625–5631.
9. Povsic,T.J. and Dervan,P. (1989) Triple helix formation by oligonucleotides on DNA extended to the physiological pH range. *J. Am. Chem. Soc.*, **111**, 3059–3061.
10. Xiang,G., Bogacki,R. and McLaughlin,L.W. (1996) Use of a pyrimidine nucleoside that functions as a bidentate hydrogen bond donor for the recognition of isolated or contiguous G-C base pairs by oligonucleotide-directed triplex formation. *Nucleic Acids Res.*, **24**, 1963–1970.
11. Ono,A., Ts'o,P.O.P. and Kan,L. (1992) Triplex formation of an oligonucleotide containing 2′-*O*-methylpseudoisocytidine with a DNA duplex at neutral pH. *J. Org. Chem.*, **57**, 3225–3230.
12. Kandimalla,E.R. and Agrawal,S. (1996) Hoogsteen DNA duplexes of 3′-3′ and 5′-5′-linked oligonucleotides and triplex formation with RNA and DNA pyrimidine single strands: experimental and molecular modeling studies. *Biochemistry*, **35**, 15332–15339.
13. van de Sande,J.H., Ramsing,N.B., Germann,M.W., Elhorst,W., Kalisch,B.W., von Kitzing,E., Pon,R.T., Clegg,R.C. and Jovin,T.M. (1988) Parallel stranded DNA. *Science*, **241**, 551–557.
14. Rippe,K. and Jovin,T.M. (1992) Parallel-stranded duplex DNA. *Methods Enzymol.*, **211**, 199–220.
15. Giovannangeli,C., Montenay-Garestier,T., Rougée,M., Chassignol,M., Thuong,N.T. and Hélène,C. (1991) Single-stranded DNA as a target for triple-helix formation. *J. Am. Chem. Soc.*, **113**, 7775–7777.
16. Rumney,S. and Kool,E.T. (1995) Structural optimisation of non-nucleotide loop replacements for duplex and triplex DNAs. *J. Am. Chem. Soc.*, **117**, 5635–5646.
17. Güimil García,R., Ferrer,E., Macías,M.J., Eritja,R. and Orozco,M. (1999) Theoretical calculations, synthesis and base pairing properties of oligonucleotides containing 8-amino-2′-deoxyadenosine. *Nucleic Acids Res.*, **27**, 1991–1998.
18. Kawai,K., Saito,I. and Sugiyama,H. (1998) Stabilization of Hoogsteen base pairing by introduction of NH_2 group at the C8 position of adenine. *Tetrahedron Lett.*, **39**, 5221–5224.
19. Rao,T.S., Durland,R.H. and Revankar,G.R. (1994) Synthesis of oligonucleotides containing 7-(2-deoxy-β-D-*erythro*-pentofuranosyl)guanine and 8-amino-2′-deoxyguanosine *J. Heterocyclic Chem.*, **31**, 935–940.
20. Rieger,R.A., Iden,C.R., Gonikberg,E. and Johnson,F. (1999) 8-Amino-2′-deoxyguanosine incorporation into oligomeric DNA. *Nucl. Nucl.*, **18**, 73–88.
21. Soliva,R., Güimil García,R., Blas,J.R., Eritja,R., Asensio,J.L., González,C., Luque,F.J. and Orozco,M. (2000) DNA-triplex stabilizing properties of 8-aminoguanine. *Nucleic Acids Res.*, **28**, 4531–4539.
22. Cubero,E., Güimil García,R., Luque,F.J., Eritja,R. and Orozco,M. (2001) The effect of amino groups on the stability of DNA duplexes and triplexes based on purines derived from inosine. *Nucleic Acids Res.*, **29**, 2522–2534.
23. Cubero,E., Aviñó,A., de la Torre,B.G., Frieden,M., Eritja,R., Luque,F.J., González,C. and Orozco,M. (2002) Hoogsteen-based parallel-stranded duplexes of DNA. The effect of 8-amino derivatives. *J. Am. Chem. Soc.*, **124**, 3133–3142.
24. Aviñó,A., Morales,J.C., Frieden,M., de la Torre,B.G., Güimil García,R., Cubero,E., Luque,F.J., Orozco,M., Azorín,F. and Eritja,R. (2001) Parallel-stranded hairpins containing 8-aminopurines. Novel efficient probes for triple-helix formation. *Bioorg. Med. Chem. Lett.*, **11**, 1761–1763.
25. Plateau,P. and Güéron,M. (1982) Exchangeable proton NMR without base-line distortion, using new strong-pulse sequences. *J. Am. Chem. Soc.*, **104**, 7310–7311.
26. Lee,C., Yang,W. and Parr,R.G. (1998) Development of the Colle-Salvetti correlation-energy formula into a functional of the electron density. *Phys. Rev. B*, **37**, 785–789.
27. Boys,S.F. and Bernardi,F. (1970) The calculation of small molecules interactions by the differences of separate total energies. Some procedures with reduced errors. *Mol. Phys.*, **19**, 553–559.
28. Shields,G., Laughton,C.A. and Orozco,M. (1997) Molecular dynamics simulations of the d(T·A·T) triple helix. *J. Am. Chem. Soc.*, **119**, 7463–7469.
29. Cubero,E., Luque,F.J. and Orozco,M. (2001) Theoretical studies of d(A:T)-based parallel-stranded DNA duplexes. *J. Am. Chem. Soc.*, **123**, 12018–12025.
30. Shields,G., Laughton,C.A. and Orozco,M. (1998) Molecular dynamics simulation of a PNA·DNA·PNA triple helix in aqueous solution. *J. Am. Chem. Soc.*, **120**, 5895–5904.
31. Darden,T.A., York,D. and Pedersen,L. (1993) Particle mesh Ewald: an N·log(N) method for Ewald sums in large systems. *J. Chem. Phys.*, **98**, 10089–10092.
32. Ryckaert,J.P., Ciccote,G. and Berendsen,J.C. (1977) Numerical integration of the Cartesian equations of motion of a system with constrains: molecular dynamics of n-alkanes. *J. Comput. Phys.*, **23**, 327–341.
33. Jorgensen,W.L., Chandrasekhar,J., Madura,J.D., Impey,R. and Klein,M.L. (1983) Comparison of single potential functions for simulating liquid water. *J. Chem. Phys.*, **79**, 926–935.
34. Cornell,W.D., Cieplak,P., Bayly,C.I., Gould,I.R., Merz,K.M., Ferguson,D.M., Spellmeyer,D.C., Fox,T., Caldwell,J.W. and Kollman,P.A. (1995) A second generation force field for the simulation of proteins, nucleic acids, and organic molecules. *J. Am. Chem. Soc.*, **117**, 5179–5197.
35. Cheatham,T.E., Cieplak,P. and Kollman,P.A. (1999) A modified version of the Cornell *et al.* force field with improved sugar pucker phases and helical repeat. *J. Biomol. Struct. Dyn.*, **16**, 845–862.
36. Soliva,R., Laughton,C.A., Luque,F.J. and Orozco,M. (1998) Molecular dynamics simulations in aqueous solution of triple helices containing d(G·C·C) trios. *J. Am. Chem. Soc.*, **120**, 11226–11233.
37. Manzini,G., Xodo,L.E. and Gasparotto,D. (1990) Triple helix formation by oligopurine-oligopyrimidine DNA fragments-electrophoretic, and thermodynamic behaviour. *J. Mol. Biol.*, **213**, 833–843.

38. Wang,S., Booher,M.A. and Kool,E.T. (1994) Stabilities of nucleotide loops bridging the pyrimidine strands in DNA pyrimidine.purine.pyrimidine triplexes: special stability of the CTTTG loop. *Biochemistry*, **33**, 4639–4644.
39. Gowers,D.M. and Fox,K.R. (1999) Towards mixed sequence recognition by triple helix formation. *Nucleic Acids Res.*, **27**, 1569–1577.
40. Venkatarangan,L., Sivaprasad,A., Jonson,F. and Basu,A.K. (2001) Site-specifically located 8-amino-2′-deoxyguanosine: thermodynamic stability and mutagenic properties in *Escherichia coli*. *Nucleic Acids Res.*, **29**, 1458–1463.
41. Sugimoto,N., Wu,P., Hara,H. and Kawamoto,Y. (2001) pH and cation effects on the properties of parallel pyrimidine motif DNA triplexes. *Biochemistry*, **40**, 9396–9405.
42. Liu,K., Miles,H.T., Frazier,J. and Sasisekharan,V. (1993) A novel DNA duplex. A parallel-stranded DNA helix with Hoogsteen base pairing. *Biochemistry*, **32**, 11802–11809.